High T_{c} via Spin Fluctuations from Incipient Bands: Application to Monolayers and Intercalates of FeSe

A. Linscheid, S. Maiti, Y. Wang, S. Johnston, and P. J. Hirschfeld

Phys. Rev. Lett. **117**, 077003 — Published 12 August 2016

DOI: 10.1103/PhysRevLett.117.077003

High T_c via spin fluctuations from incipient bands: application to monolayers and intercalates of FeSe

A. Linscheid,[1] S. Maiti,[1] Y. Wang,[2] S. Johnston,[2] and P. J. Hirschfeld[1]

[1] *Department of Physics, University of Florida, Gainesville,FL 32611*

[2] *Department of Physics and Astronomy, University of Tennessee, Knoxville, Tennessee 37996*

(Dated: May 9, 2016)

We investigate superconductivity in a two-band system with an electron- and a hole-like band, where one of the bands is away from the Fermi level (or "incipient"). We argue that the incipient band contributes significantly to spin-fluctuation pairing in the strong coupling limit where the system is close to a magnetic instability, and can lead to a large T_c. In this case, T_c is limited by a competition between the frequency range of the coupling (set by an isolated paramagnon) and the coupling strength itself, such that a dome-like T_c dependence on the incipient band position is obtained. The coupling of electrons to phonons is found to further enhance T_c. The results are discussed in the context of experiments on monolayers and intercalates of FeSe.

Introduction Iron based superconductors (FeSC) form the largest family of unconventional superconductors (SC) known to us. This includes the stoichiometric, pressurized, doped and/or intercalated versions of quasi-2D layered Fe-pnictogen or Fe-chalcogen compounds. These systems host a variety of superconducting phases and exhibit a broad range of T_c's [1–4], which still lack a consistent explanation. Among these, the FeSe systems present a curious phenomenology: almost all members related to this family –alkali/alkali-hydroxy intercalated FeSe [5–7], ammonia intercalated FeSe [8–11]– exhibit $T_c \sim 35-45$ K and even reaching $60-70$ K in the case of single unit cell (UC) thick FeSe grown on 001-$SrTiO_3$ (STO) [12–15], 110-STO, and [16, 17] 001-$BaTiO_3$ (BTO) [18]. Even bulk FeSe, which has a T_c of only 8 K [19], exhibits a maximum T_c of 36 K [20] under pressure.

The relatively high T_c's in these systems have been correlated with an increase of the *ab*-plane lattice constant in multi UC FeSe films [21, 22] or an increase in the *c*-axis lattice constant in the intercalates [22, 23]. The evolution from single- to multi-UC films is not smooth [24], but the general trend is that T_c is suppressed when more layers are added. Another correlation, particular to the 1 UC FeSe on STO (and BTO), is based on the observation of 'replica' bands ~ 100 meV below the electron and hole bands [15]. This indicates a strong forward-focused ($\boldsymbol{q}=0$) electron-phonon (e-ph) coupling to a polar phonon mode of the doped STO substrate, which was recently invoked to explain the high T_c of the interfaces [15, 25–27].

This, however, does not explain the relatively high T_c in the other FeSe systems without substrates, nor why electron doping and removing the hole Fermi pockets generally enhances T_c [2, 28]. This trend also appears to directly contradict the spin fluctuation (SF) pairing scenario for FeSC, where the pair scattering by repulsive interactions between hole and electron Fermi pockets (separated by $\mathbf{Q}$) leads to strong pairing; naively, removing the hole pocket should suppress T_c rapidly. Indeed, while a recent work on incipient band pairing showed that if pairing exists, making use of electronic states at the Fermi level (FL), superconductivity can also be induced in incipient bands [29], the authors also found that moving the hole band away from the FL always suppresses T_c. These results, however, are based on static, band structure independent interactions. Here, we show that this conclusion is different if dynamical interactions near a magnetic instability are used.

We note that the monolayer and intercalate FeSe systems have electron-like Fermi pockets at the $M-$points, and an incipient hole band $50-100$ meV below the FL at Γ [5, 12–15]. This incipient hole band, neglected in nearly all analyses of SC pairing, is shown here to play a crucial role in the strong coupling regime and supports simple $s_\pm$ pairing.

Since the anomalous FeSe systems are generally tetragonal and quasi-2D, we adopt a two band system with a regular electron band and incipient hole band. We solve Eliashberg-type equations where pairing is mediated by the interband SF, considered in the strong coupling regime close to a magnetic instability. We argue that the FeSe systems are able to sustain stronger electronic correlations without developing magnetic long range order due to the suppression of interband scattering by the incipient electronic states.

The proximity to magnetism is well established in these systems. In fact, the interpretation of the data in Refs. [21] and [28] suggests that the FeSe film thickness of as low as 3 UC on STO has a hole band crossing the FL, accompanied by spectral features associated with a magnetic state. A large T_c is recovered by electron doping [28]. Further, a first principles study [30] of 1 UC FeSe/STO found that FeSe would have a very strong spin-density wave (SDW) without the substrate induced electron doping, again suggesting strong correlations in the system.

We find that the pairing is dominated by a paramagnon

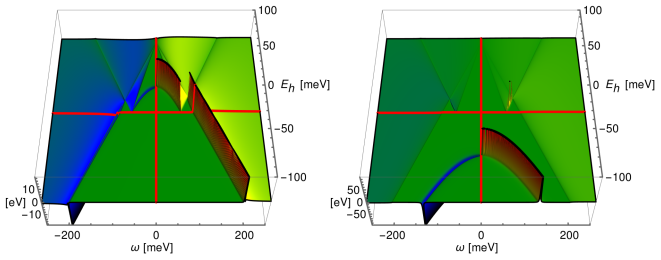

Figure 1. (color online) Imaginary part of $V^{\rm SF}(\boldsymbol{Q},\omega+\mathrm{i}\eta)$ for $U=0.325$eV(left) and $U=0.5$eV(right) and $\Lambda_{\rm B}=2$eV. The Lifshitz transition $E_{\rm h}=0$ and zero energy $\omega=0$ are red lines.

peak in the SF propagator at an energy $\Omega_{\rm p}$. Due to the electronic origin of the bosonic peak, its position controls both the pairing bandwidth and the coupling strength. As the peak hardens, the interplay between quantities results in a non-monotonic behavior of T_c such that pushing the band deeper below the E_F *increases* T_c. Introducing an additional e-ph coupling further enhances T_c [29].

Model We take the electron and hole band dispersions as ($\hbar=1$)

$$\varepsilon^{\rm h}_{\boldsymbol{k}}=-\frac{\boldsymbol{k}^2}{2m^*_{\rm h}}+E_{\rm h},\qquad \varepsilon^{\rm e}_{\boldsymbol{k}}=\frac{(\boldsymbol{k}-\boldsymbol{Q})^2}{2m^*_{\rm e}}+E_{\rm e}, \tag{1}$$

where $m^*_{\rm e}$ ($m^*_{\rm h}$) is the effective electron (hole) band mass, $E_{\rm e}$ ($E_{\rm h}$) is the electron (hole) band extrema measured relative to the chemical potential μ, and $\boldsymbol{Q}$ is the wavevector at which SFs are peaked. The bandwidth is set by requiring the bands to extend up to $\Lambda_{\rm B}$ around their respective centers in momentum space. We convert all momenta in our plots to energy using $m^*_{\rm h}$. In all numerical plots we fix $\Lambda_B=900$ meV and $E_e=-60$ meV, unless otherwise specified.

In the SF framework, the bosonic propagator mediating pairing is the transverse interband spin susceptibility $\chi^{\uparrow\downarrow}_{\rm he}(\boldsymbol{q},\mathrm{i}\nu_n)$ (we henceforth drop the spin indices). Under the usual FLEX-based approximations [31–34], the susceptibility acquires a Stoner-like enhancement and the propagator can be modeled as

$$V^{\rm SF}(\boldsymbol{q},\mathrm{i}\nu_n)=\frac{U^2\left(\chi^0_{\rm he}(\boldsymbol{q},\mathrm{i}\nu_n)+\chi^0_{\rm eh}(\boldsymbol{q},\mathrm{i}\nu_n)\right)}{1-U\left(\chi^0_{\rm he}(\boldsymbol{q},\mathrm{i}\nu_n)+\chi^0_{\rm eh}(\boldsymbol{q},\mathrm{i}\nu_n)\right)},\qquad \text{where}$$
$$\chi^0_{\rm he}(\boldsymbol{q},\mathrm{i}\nu_n)=-\int\frac{\mathrm{d}^2\boldsymbol{k}}{4\pi^2}\frac{f(\varepsilon^{\rm h}_{\boldsymbol{k}})-f(\varepsilon^{\rm e}_{\boldsymbol{k}+\boldsymbol{q}})}{\mathrm{i}\nu_n+\varepsilon^{\rm h}_{\boldsymbol{k}}-\varepsilon^{\rm e}_{\boldsymbol{k}+\boldsymbol{q}}}=\chi^0_{\rm eh}(\boldsymbol{q},-\mathrm{i}\nu_n). \tag{2}$$

Here, f is the Fermi function and $U>0$ is a repulsive point-contact interaction parameter that has the same scale as those in Hubbard-Hund type models [32, 33]. Note that we are discarding the remaining charge and spin susceptibilities that arise in the FLEX formalism. We likely overestimate T_c in this approach.

In the weak coupling limit $u\equiv m^*_{\rm e}m^*_{\rm h}U/2\pi(m^*_{\rm e}+m^*_{\rm h})\ll 1$, for the incipient case $E_{\rm h}<0$, the propagator $V^{\rm SF}$ is nonsingular and can be treated as a constant [29]. For $u\sim 1$, however, the system hosts a sharp paramagnon peak (a pole at $\Omega=\Omega_{\rm p}$ in the retarded $V^{\rm SF}$) controlled by $E_{\rm h}$ (see Fig. 1). The position of this peak determines not only the size of the electron-SF coupling but also the 'pairing bandwidth' $\Lambda_{\rm SF}$ over which the pairing interaction acts.

An estimate for T_c Before solving the Eliashberg equations we offer a qualitative picture of the interplay between the coupling and the pairing bandwidth $\Lambda_{\rm SF}$. To proceed, we focus on $\boldsymbol{q}=\boldsymbol{Q}$. Assuming also $E_{\rm h}<0$, $\Lambda_{\rm B}\gg E_{\rm h,e}$ and $T=0$, we obtain

$$\chi^0_{\rm he}(\boldsymbol{Q},\Omega_{\rm p})=-\frac{m^*_{\rm e}}{2\pi(r+1)}\ln[\frac{r|E_{\rm e}|+|E_{\rm h}|+\Omega_{\rm p}}{\Lambda_{\rm B}(1+r)}], \tag{3}$$

where $r=m^*_{\rm e}/m^*_{\rm h}$. It is clear from Eq. (2) that a magnetic instability sets in for $U=U_c\equiv 1/\left[\chi^0_{\rm he}(\boldsymbol{Q},0)+\chi^0_{\rm eh}(\boldsymbol{Q},0)\right]$. For $U<U_c$, we then have a paramagnon peak at

$$\Omega^2_{\rm p}=(|E_{\rm h}|+r|E_{\rm e}|)^2-E_0^2\to 2E_0(E^*_{\rm h}-E_{\rm h}), \tag{4}$$

where the paramagnon softens at $E_{\rm h}=E^*_{\rm h}\equiv -E_0+r|E_{\rm e}|$ and $E_0\equiv\Lambda_{\rm B}(1+r)\mathrm{e}^{-\frac{1}{2u}}$.

The dimensionless electron-boson coupling $v_{\rm SF}$ is obtained from the static limit of the bosonic propagator multiplied by density of states, and the bandwidth of the pairing interaction $\Lambda_{\rm SF}$ is the energy of the bosonic mode $\Omega_{\rm p}$. Thus,

$$V^{\rm stat}_{\rm SF}(\boldsymbol{Q})=U\frac{uR}{1-uR}\to U\frac{E_0}{|E_{\rm h}-E^*_{\rm h}|}, \tag{5}$$

with $R=-2\ln\left[|rE_{\rm e}+E_{\rm h}|/\Lambda_{\rm B}(1+r)\right]$ and $v^{\rm e/h}_{\rm SF}=V^{\rm stat}_{\rm SF}m^*_{\rm e/h}/2\pi$. To get an estimate for T_c, we note that as a function of $E_{\rm h}$, the coupling $V^{\rm stat}_{\rm SF}$ varies from $V^{\rm stat}_{\rm SF}\gg 1$ near $E^*_{\rm h}$ to $V^{\rm stat}_{\rm SF}\ll 1$ far from $E^*_{\rm h}$ (see Fig. 2b). For $v^{e/h}_{\rm SF}\ll 1$ and $\Lambda_{\rm SF}>|E_h|$, T_c is given by $\Lambda_{\rm SF}\exp\{-1/[v^{\rm e}_{\rm SF}v^{\rm h}_{\rm SF}\ln(\Lambda_{\rm SF}/|E_h|)]\}$, which is from Ref. 29, where in the present work we account for the E_h dependence of $\Lambda_{\rm SF}$ and $v_{\rm SF}$. For $v_{\rm SF}\gg 1$, T_c has the Allen-Dynes [35] lower bound given by $\Lambda_{\rm SF}(v^{\rm e}_{\rm SF}v^{\rm h}_{\rm SF})^{1/4}$. Near the instability, Eqs. (4) and (5) yield that the couplings $v^{\rm e/h}_{\rm SF}$ diverge as $1/|E_{\rm h}-E^*_{\rm h}|$ and $\Lambda_{\rm SF}$ vanishes as $\sqrt{|E_{\rm h}-E^*_{\rm h}|}$. We obtain the lower bound

$$T_c\gtrsim E_0\left(\frac{m^*_{\rm e}+m^*_{\rm h}}{\sqrt{m^*_{\rm e}m^*_{\rm h}}}\right)^{1/2}. \tag{6}$$

If the coupling diverges, it is tempting to conclude that $T_c\to\infty$ within Eliashberg theory. However, we have demonstrated that even within an Eliashberg type theory, T_c may remain finite. The schematic evolution of T_c with $E_{\rm h}$ based on these considerations is presented in Fig. 2a. The suppression of T_c near $E^*_{\rm h}$ is a consequence of the dynamics of the pairing interaction, leading to a strong mass renormalization of quasiparticles in the Fermi-liquid state.

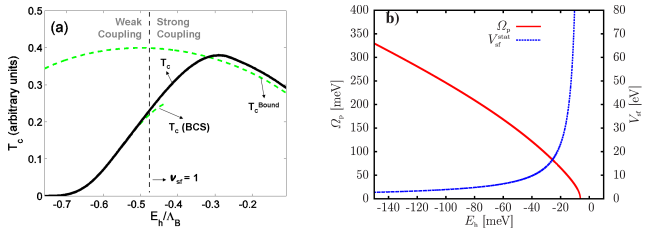

Figure 2. (Color online) a) Schematic T_c of E_h. T_c interpolates between the BCS behavior in the weak coupling regime ($v_\mathrm{SF} \ll 1$) and the strong coupling lower bound for $v_\mathrm{SF} \gg 1$). b) The paramagnon and the static propagator V_SF^{stat} ($U = 0.45$ eV). Here $m_\mathrm{e}^* = 2.6m_e$ and $m_\mathrm{h}^* = 1.6m_e$.

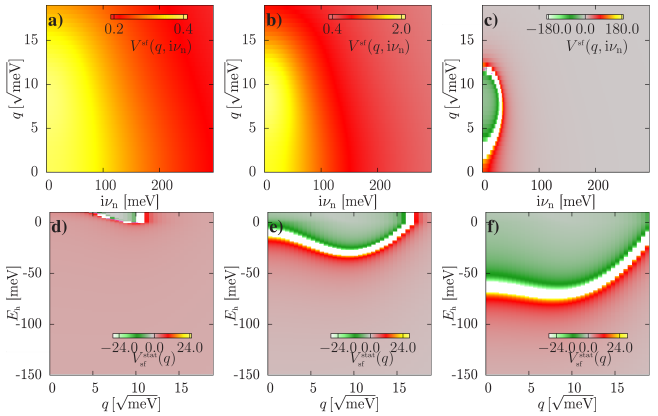

Figure 3. (color online) Momentum dependence of $V^\mathrm{SF}(q, \mathrm{i}\nu_n)$ at $E_\mathrm{h} = -65$ meV for $U = 0.45, 0.6$ and 0.7 eV in a), b) and c) and of the static part $V_\mathrm{SF}^\mathrm{stat}(q)$ for $U = 0.45, 0.6$ and 0.7 eV in d), e) and f) as a function Matsubara frequency and doping E_h. q measures the deviation form $\boldsymbol{Q}$.

Incipient Eliashberg equations To accurately describe the region close to the instability E_h^*, we need to solve the Eliashberg equations. These can be greatly simplified if the effective interaction V^SF does not depend strongly on $\boldsymbol{q}$. In Fig. 3 we investigate this dependence around $\boldsymbol{Q}$, defining $\tilde{\boldsymbol{q}} = \boldsymbol{Q}+\boldsymbol{q}$. The Stoner-like enhancement leads to a strong variation of $V^\mathrm{SF}(\boldsymbol{q}, \mathrm{i}\nu_n = 0)$ close to the instability, as can be seen in Figs. 3a) - 3c). In Fig. 3d), 3e) and 3f) we show $V^\mathrm{SF}(\boldsymbol{q}, 0)$ as a function of E_h and the momentum deviation q for the interaction parameters $U = 0.45$, 0.6, and 0.7 eV, respectively. The regions shown in green are beyond the instability and correspond to a magnetic ground state. Thus, in Fig. 3c), the magnetic instability occurs at a finite q leading to an incommensurate SDW ground state. As is evident in Fig. 3, the momentum dependence is only important very close to the instability and is featureless when the hole band goes deeper below the FL; we conclude that the $\boldsymbol{q}$ can be neglected in this region of parameter space.

The multiband isotropic Eliashberg equations in Matsubara axis are:

$$Z_{n,i} = 1 + \frac{T}{\omega_n}\sum_{n'i'}[\lambda^\mathrm{ph}_{n-n';i,i'}\xi^\mathrm{ph}_{n',i'} + \lambda^{SF}_{n-n';i,i'}\xi^\mathrm{SF}_{n',i'}]\omega_{n'}$$

$$Z_{n,i}\Delta_{n,i} = T\sum_{n'i'}[\lambda^\mathrm{ph}_{n-n';i,i'}\xi^\mathrm{ph}_{n',i'} - \lambda^\mathrm{SF}_{n-n';i,i'}\xi^\mathrm{SF}_{n',i'}]\Delta_{n',i'}.$$

Here, $i, i' \in \{\mathrm{h},\mathrm{e}\}$; $\xi^\mathrm{P}_{n,i} = \int_{l_\mathrm{P}}^{h_\mathrm{P}} \mathrm{d}\varepsilon/D_{n,i}$, with $D_{n,i} = \varepsilon^2 + Z^2_{n,i}(\omega_n^2 + |\Delta_{n,i}|^2)$ and l_P, h_P being the cut-offs set by the mechanism $\mathrm{P} \in \{\mathrm{ph}, \mathrm{SF}\}$. Furthermore $\lambda^\mathrm{SF}_{n-n';i,i'} = N_{i'}V^\mathrm{SF}(\boldsymbol{Q}, \mathrm{i}\omega_n - \mathrm{i}\omega_{n'})\delta_{i,\bar{i}'}$, where $N_\mathrm{h,e}$ are the density of states of the electron and hole bands; and $\lambda^\mathrm{ph}_{n-n';i,i'} = \int \mathrm{d}\Omega\, 2\Omega\alpha^2F_{i,i'}(\Omega)/[(\omega_n-\omega_{n'})^2+\Omega^2]$. We have neglected the single-particle energy renormalization $\chi_{n,i}$.

For the following numerical solution, we choose experimental parameters for FeSe on $SrTiO_3$ from Ref. [36]: $m_\mathrm{h}^* = 1.6m_\mathrm{e}$, $m_\mathrm{e}^* = 2.6m_\mathrm{e}$, lattice constant $a = 3.9$ Å, and $E_\mathrm{e} = -60$ meV. In Fig. 4, we show the numerical solution to the Eliashberg equations. Fig. 4a), shows the gap $\Delta(i\pi T)$ as a function of temperature and electron doping (E_h). For the given $\Lambda_\mathrm{B} = 900$ meV, we observe a maximum T_c at about the experimental position of the hole band ($E_\mathrm{h}^\mathrm{exp} = -78$ meV [36]) if we assume a reasonable interaction parameter of $U = 0.7$ eV.

Figures 4d) and 4e) show the temperature and doping dependence of the two $s_\pm$ gaps, respectively. Note that the interband nature of the interaction makes the incipient hole gap larger than the electron band gap. This explains the counterintuitive trend in Fig. 4d) whereby the electron band gap is suppressed faster by continued electron doping while the hole band gap reaches its maximum at lower E_h.

Figure 4f) plots the ratio $2\Delta_{\mathrm{e,h}}/T_c$. For E_h far away from the instability, we find the BCS value of $2\Delta_\mathrm{e}/T_c = 3.5$. This value increases as E_h moves towards E_h^* to about 9, reflecting the strong coupling behavior near the magnetic instability. $2\Delta_\mathrm{h}/T_c$ has a similar behavior close to the instability, but is also much larger than the electron band ratio far from the instability.

The overestimation of T_c Our model allows T_c values well above 200 K. Note, however, that we have neglected the intraband component of the repulsive interactions that will reduce this estimate. This is typically captured by the μ^* approximation. While one can show that an analogous RPA treatment leads to a Coulomb repulsion screened by the electron-band susceptibility, the use of the μ^* approximation is questionable due to the shallowness of the electron band. A more accurate calculation of this contribution requires momentum resolution, which would increase the complexity of our model. Thus, we leave this for future work. Finally, T_c is also likely suppressed in the real system due to increased fluctuations in 2D that are beyond the Eliashberg formalism.

Role of phonons Since the momentum dependence of the interactions is neglected here, we cannot account for strong small $\mathbf{q}$ nature of the e-ph interaction in the 1UC

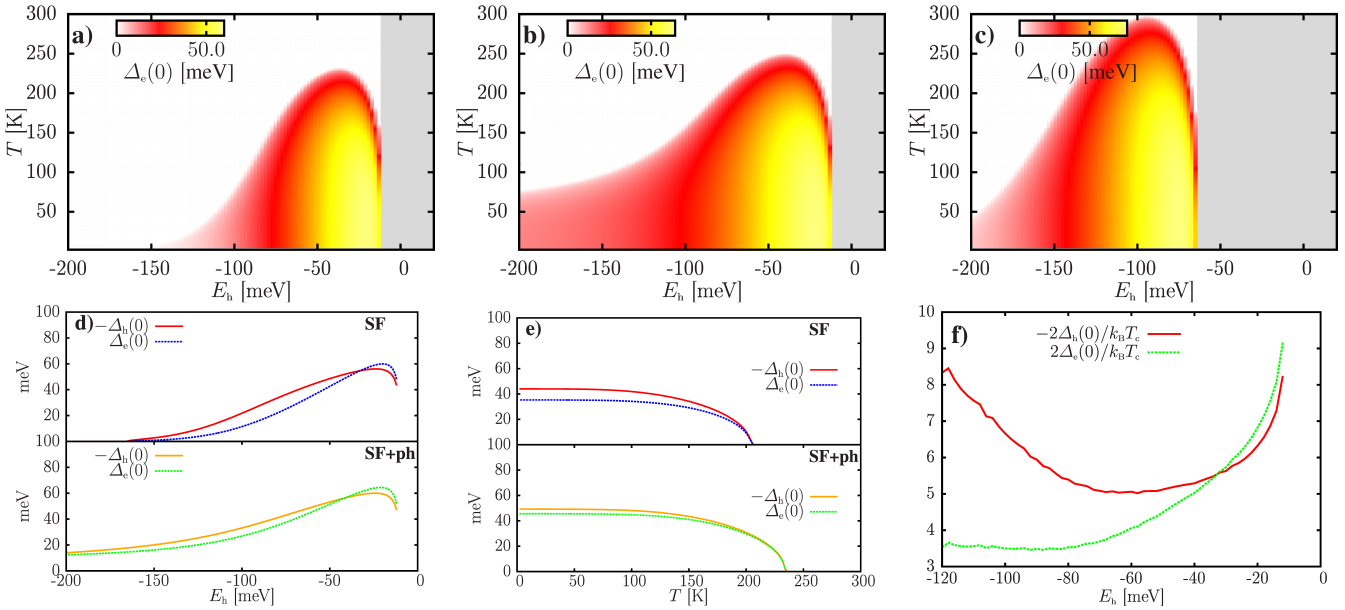

Figure 4. (color online) $\Delta_e(0)$ as a function of E_h and T in a) via SF ($U = 0.6$) and in b) with an additional intraband phonon interaction of $\lambda_{ph} = 0.6$ and $\omega_{ph} = 100$ meV c) same as a) but with U increased to 0.7 eV. Shaded areas in a), b) and c) are antiferromagnetic. d) gaps as a function of doping at $T = 2$ K (top) and with the additional phonon interaction (bottom). e) gaps as a function of T (top) and with the additional phonon interaction (bottom) at $E_h = -60$ meV. f) Gap ratios for electron and hole gap vs. E_h.

FeSe/STO; however, this coupling will lead to a purely attractive intraband interaction. We therefore add in Fig. 4b) an intraband phonon interaction with $\lambda_{ph} = 0.6$, $\Omega_{ph} = 100$ meV, and $\alpha^2 F_{i,i'}(\Omega) = \frac{\lambda_{ph}\Omega_{ph}}{2}\delta_{i,i'}\delta(\Omega - \Omega_{ph})$. (These parameters are motivated by estimates obtained from experiments [15, 25].) This additional interaction increases T_c^{max} to 250 K at the optimal E_h and makes superconductivity persist to much lower E_h. We note that the repulsive intraband interaction will reduce the overall electronic coupling in the $s_\pm$ channel and make the attractive phonon interaction more significant.

Conclusions We have shown that when a magnetic instability nearly coincides with a band moving below the FL, this so-called incipient band can support $s_\pm$ pairing with a fully gapped SC state at the FL. Within a simple two-band model, T_c has a dome-like behavior due to the competition between the coupling strength and SF bandwidth. Both of these are controlled by the paramagnon peak in the SF spectrum, which is present for systems with strong correlations ($u \sim 1$). For weakly correlated systems ($u \ll 1$), there is no such peak and one recovers the results of Ref. 29. With realistic values for the parameters, we find significant T_c's, even in the absence of Fermi surface-based interactions. In particular, For values relevant to FeSe monolayers and intercalates, we find that the maximum T_c is clearly capable of explaining the high critical temperatures observed in these systems. Including an additional phonon coupling in the energy range of the suspected oxygen modes of STO observed in Ref. [15] further enhances T_c.

This spin-fluctuation mechanism differs from all the Fermi-surface based models discussed previously [31–34] due to the presence of the incipient band; while static theories would predict no SC within the model we have considered, accounting for the dynamics of excitations allowed by the incipient band leads to high-T_c pairing.

The authors are grateful for useful discussions with T. Maier, V. Mishra, and D.J. Scalapino. PJH and AL were supported by DE-FG02-05ER46236. S. J. and Y. W. are partially funded by the University of Tennessee's Science Alliance Joint Directed Research and Development (JDRD) program, a collaboration with Oak Ridge National Laboratory.

[1] A. Chubukov and P. J. Hirschfeld, Physics Today **68**, 46 (2015).
[2] P. J. Hirschfeld, Comptes Rendus Physique **17**, 197 (2016).
[3] A. Chubukov, Annual Review of Condensed Matter Physics **3**, 57 (2012).
[4] H.-H. Wen and S. Li, Annual Review of Condensed Matter Physics **2**, 121 (2011).
[5] T. Qian, X.-P. Wang, W.-C. Jin, P. Zhang, P. Richard, G. Xu, X. Dai, Z. Fang, J.-G. Guo, X.-L. Chen, and H. Ding, Physical review letters **106**, 187001 (2011).
[6] X. H. Niu, R. Peng, H. C. Xu, Y. J. Yan, J. Jiang, D. F. Xu, T. L. Yu, Q. Song, Z. C. Huang, Y. X. Wang, B. P. Xie, X. F. Lu, N. Z. Wang, X. H. Chen, Z. Sun, and D. L. Feng, Physical Review B **92**, 060504 (2015).

[7] L. Zhao, A. Liang, D. Yuan, Y. Hu, D. Liu, J. Huang, S. He, B. Shen, Y. Xu, X. Liu, L. Yu, G. Liu, H. Zhou, Y. Huang, X. Dong, F. Zhou, K. Liu, Z. Lu, Z. Zhao, C. Chen, Z. Xu, and X. J. Zhou, Nature Communications **7**, 10608 (2016).

[8] J. Guo, H. Lei, F. Hayashi, and H. Hosono, Nature communications **5**, 4756 (2014).

[9] S. J. Sedlmaier, S. J. Cassidy, R. G. Morris, M. Drakopoulos, C. Reinhard, S. J. Moorhouse, D. O'Hare, P. Manuel, D. Khalyavin, and S. J. Clarke, Journal of the American Chemical Society **136**, 630 (2014).

[10] M. Burrard-Lucas, D. G. Free, S. J. Sedlmaier, J. D. Wright, S. J. Cassidy, Y. Hara, A. J. Corkett, T. Lancaster, P. J. Baker, S. J. Blundell, and S. J. Clarke, Nature materials **12**, 15 (2013).

[11] D. Guterding, H. O. Jeschke, P. J. Hirschfeld, and R. Valentí, Physical Review B **91**, 041112 (2015).

[12] Q.-Y. Wang, Z. Li, W.-H. Zhang, Z.-C. Zhang, J.-S. Zhang, W. Li, H. Ding, Y.-B. Ou, P. Deng, K. Chang, J. Wen, C.-L. Song, K. He, J.-F. Jia, S.-H. Ji, Y.-Y. Wang, L.-L. Wang, X. Chen, X.-C. Ma, and Q.-K. Xue, Chinese Physics Letters **29**, 037402 (2012).

[13] D. Liu, W. Zhang, D. Mou, J. He, Y.-B. Ou, Q.-Y. Wang, Z. Li, L. Wang, L. Zhao, S. He, Y. Peng, X. Liu, C. C. Chen, L. Yu, G. Liu, X. Dong, J. Zhang, C. C. Chen, Z. Xu, J. Hu, X. Chen, X. Ma, Q. Xue, and X. Zhou, Nature Communications **3**, 931 (2012), arXiv:1202.5849.

[14] S. He, J. He, W. Zhang, L. Zhao, D. Liu, X. Liu, D. Mou, Y.-B. Ou, Q.-Y. Wang, Z. Li, L. Wang, Y. Peng, Y. Liu, C. Chen, L. Yu, G. Liu, X. Dong, J. Zhang, C. Chen, Z. Xu, X. Chen, X. Ma, Q. Xue, and X. J. Zhou, Nature Materials **12**, 605 (2013).

[15] J. J. Lee, F. T. Schmitt, R. G. Moore, S. Johnston, Y.-T. Cui, W. Li, M. Yi, Z. K. Liu, M. Hashimoto, Y. Zhang, D. H. Lu, T. P. Devereaux, D.-H. Lee, and Z.-X. Shen, Nature **515**, 245 (2014).

[16] P. Zhang, X. L. Peng, T. Qian, P. Richard, X. Shi, J. Z. Ma, B. B. Fu, Y. L. Guo, Z. Q. Han, S. C. Wang, L. L. Wang, Q. K. Xue, J. P. Hu, Y. J. Sun, and H. Ding, (2015), arXiv:1512.01949.

[17] G. Zhou, D. Zhang, C. Liu, C. Tang, X. Wang, Z. Li, C. Song, S. Ji, K. He, L. Wang, X. Ma, and Q.-K. Xue, (2015), arXiv:1512.01948.

[18] R. Peng, H. C. Xu, S. Y. Tan, H. Y. Cao, M. Xia, X. P. Shen, Z. C. Huang, C. H. P. Wen, Q. Song, T. Zhang, B. P. Xie, X. G. Gong, and D. L. Feng, Nature communications **5**, 5044 (2014).

[19] F.-C. Hsu, J.-Y. Luo, K.-W. Yeh, T.-K. Chen, T.-W. Huang, P. M. Wu, Y.-C. Lee, Y.-L. Huang, Y.-Y. Chu, D.-C. Yan, and M.-K. Wu, Proceedings of the National Academy of Sciences **105**, 14262 (2008).

[20] S. Medvedev, T. M. McQueen, I. a. Troyan, T. Palasyuk, M. I. Eremets, R. J. Cava, S. Naghavi, F. Casper, V. Ksenofontov, G. Wortmann, and C. Felser, Nature materials **8**, 630 (2009), arXiv:0903.2143.

[21] S. Tan, Y. Zhang, M. Xia, Z. Ye, F. Chen, X. Xie, R. Peng, D. Xu, Q. Fan, H. Xu, J. Jiang, T. Zhang, X. Lai, T. Xiang, J. Hu, B. Xie, and D. Feng, Nature Materials **12**, 634 (2013).

[22] X. Liu, L. Zhao, S. He, J. He, D. Liu, D. Mou, B. Shen, Y. Hu, J. Huang, and X. J. Zhou, Journal of Physics: Condensed Matter **27**, 183201 (2015).

[23] T. Noji, T. Hatakeda, S. Hosono, T. Kawamata, M. Kato, and Y. Koike, Physica C: Superconductivity **504**, 8 (2014).

[24] X. Liu, D. Liu, W. Zhang, J. He, L. Zhao, S. He, D. Mou, F. Li, C. Tang, Z. Li, L. Wang, Y. Peng, Y. Liu, C. Chen, L. Yu, G. Liu, X. Dong, J. Zhang, C. Chen, Z. Xu, X. Chen, X. Ma, Q. Xue, and X. J. Zhou, Nature Communications **5**, 5047 (2014).

[25] L. Rademaker, Y. Wang, T. Berlijn, and S. Johnston, New Journal of Physics **18**, 022001 (2016).

[26] Y. Wang, K. Nakatsukasa, L. Rademaker, T. Berlijn, and S. Johnston, (2016), arXiv:1602.00656.

[27] Z.-X. Li, F. Wang, H. Yao, and D.-H. Lee, , 5 (2015), arXiv:1512.06179.

[28] Y. Miyata, K. Nakayama, K. Sugawara, T. Sato, and T. Takahashi, Nature Materials **14**, 775 (2015).

[29] X. Chen, S. Maiti, A. Linscheid, and P. J. Hirschfeld, Physical Review B **92**, 224514 (2015).

[30] K. Liu, Z.-Y. Lu, and T. Xiang, Physical Review B **85**, 235123 (2012).

[31] N. F. Berk and J. R. Schrieffer, Physical Review Letters **17**, 433 (1966).

[32] N. E. Bickers, D. J. Scalapino, and S. R. White, Phys. Rev. Lett. **62**, 961 (1989).

[33] S. Graser, T. A. Maier, P. J. Hirschfeld, and D. J. Scalapino, New Journal of Physics **11**, 025016 (2009), arXiv:0812.0343.

[34] F. Essenberger, A. Sanna, A. Linscheid, F. Tandetzky, G. Profeta, P. Cudazzo, and E. K. U. Gross, Physical Review B **90**, 214504 (2014).

[35] P. B. Allen and R. C. Dynes, Physical Review B **12**, 905 (1975).

[36] Y. Fang, D. H. Xie, W. Zhang, F. Chen, W. Feng, B. P. Xie, D. L. Feng, X. C. Lai, and S. Y. Tan, , 8 (2015), arXiv:1511.05418.